



An Improved Representation of Fire Non-Methane Organic Gases (NMOGs) in Models: Emissions to Reactivity

5 Therese S. Carter¹, Colette L. Heald^{1,2}, Jesse H. Kroll¹, Eric C. Apel³, Donald Blake⁴, Matthew Coggon⁵, Achim Edtbauer⁶, Georgios Gkatzelis^{5,7,#}, Rebecca S. Hornbrook³, Jeff Peischl^{5,7}, Eva Y. Pfannerstill^{6*}, Felix Piel^{8,9}, Nina G. Reijrink^{6,10}, Akima Ringsdorf⁶, Carsten Warneke⁵, Jonathan Williams⁶, Armin Wisthaler^{9,11}, and Lu Xu^{12,**}

¹Civil and Environmental Engineering Department, Massachusetts Institute of Technology, Cambridge, MA 02139, USA

10 ²Earth, Atmospheric and Planetary Sciences, Massachusetts Institute of Technology, Cambridge, MA 02139, USA

³Atmospheric Chemistry Observations & Modeling Laboratory, National Center for Atmospheric Research, Boulder, CO 80301, USA

⁴Chemistry Department, University of California Irvine 92697

15 ⁵NOAA Chemical Sciences Laboratory, Boulder, CO, 80305, USA

⁶Atmospheric Chemistry Department, Max Planck Institute for Chemistry, 55128, Mainz, Germany

⁷Cooperative Institute for Research in Environmental Sciences, University of Colorado Boulder, Boulder, CO, USA

20 ⁸Ionicon Analytik, Innsbruck, Austria

⁹Department of Chemistry, University of Oslo, Oslo, Norway

¹⁰IMT Nord Europe, Institut Mines-Télécom, Univ. Lille, Center for Energy and Environment, F-59000 Lille, France

¹¹Institute for Ion Physics and Applied Physics, University of Innsbruck, Innsbruck, Austria

25 ¹²Division of Geological and Planetary Sciences, California Institute of Technology, Pasadena, CA, USA

Now at: Institute of Energy and Climate Research, IEK-8: Troposphere, Forschungszentrum Jülich GmbH, Jülich, Germany

30 *Now at: Department of Environmental Science, Policy, and Management, University of California, Berkeley, CA 94720, USA

**Now at: 7 and 5

Correspondence: Therese S. Carter (tscarter@mit.edu) and Colette L. Heald (heald@mit.edu)

Abstract.



Fires emit a substantial amount of non-methane organic gases (NMOGs); the atmospheric
35 oxidation of which can contribute to ozone and secondary particulate matter formation.
However, the abundance and reactivity of these fire NMOGs are uncertain and historically not
well constrained. In this work, we expand the representation of fire NMOGs in a global chemical
transport model, GEOS-Chem. We update emission factors to Andreae (2019) and the chemical
mechanism to include recent aromatic and ethene/ethyne model improvements (Bates et al.,
40 2021; Kwon et al., 2021). We expand the representation of NMOGs by adding lumped furans to
the model (including their fire emission and oxidation chemistry) and by adding fire emissions of
nine species already included in the model, prioritized for their reactivity using data from the
FIREX laboratory studies. Based on quantified emissions factors, we estimate that our improved
representation captures 72% of emitted, identified NMOG carbon mass and 49% of OH
45 reactivity from savanna and temperate forest fires, a substantial increase from the standard model
(49% of mass, 28% of OH reactivity). We evaluate fire NMOGs in our model with observations
from the Amazon Tall Tower Observatory (ATTO), FIREX-AQ and DC3 in the US, and
ARCTAS in boreal Canada. We show that NMOGs, including furan, are well simulated in the
eastern US with some underestimates in the western US and that adding fire emissions improves
50 our ability to simulate ethene in boreal Canada. We estimate that fires provide 15% of annual
mean simulated surface OH reactivity globally, and exceeding 75% over fire source regions.
Over continental regions about half of this simulated fire reactivity comes from NMOG species.
We find that furans and ethene are important globally for reactivity, while phenol is more
important at a local level in the boreal regions. This is the first global estimate of the impact of
55 fire on atmospheric reactivity.

1 Introduction

Biomass burning (both wildfires and prescribed and agricultural burns) is a large source of non-
methane organic gases (NMOGs) (e.g., Akagi et al., 2011; Koss et al., 2018; Coggon et al., 2019;
60 Kumar et al., 2018). Goldstein and Galbally (2007) suggest that, while tens of thousands of
organic compounds have been detected in the atmosphere, this may represent only a small subset
of the species present in the atmosphere. Only ~100 compounds have typically been measured
during field campaigns, but recent advances in mass spectrometry have enabled the online



65 characterization of an expanding suite of organic compounds in the atmosphere, including those
from fires (e.g., Koss et al., 2018). Because many NMOGs are quite reactive, they impact
tropospheric and stratospheric (Bernath et al., 2022) chemistry and composition. Many NMOGs
are toxic themselves (Naeher et al., 2007), and they can also react to form two major air
pollutants that are also harmful to human health, ozone (O₃) and particulate matter under 2.5
microns (PM_{2.5}) (e.g., Hobbs et al., 2003; Yokelson et al., 2009; Jaffe et al., 2008, 2013, 2018; Xu
70 et al., 2021). NMOGs also modulate oxidant concentrations, which affect the climate through the
methane lifetime (Voulgarakis et al., 2013). The importance of fires to the budget of global
NMOGs and to the impacts discussed above is not well understood, as suggested by a recent
study (Bourgeois et al., 2021).

75 Various terms have been used in the literature to describe reactive carbon-containing trace gases,
including one of the first, non-methane hydrocarbons (NMHCs), which excludes species with
oxygen or other heteroatoms. The term volatile organic compounds (VOCs) encompasses this
broader set of compounds; although, there is no agreed upon, quantitative definition for VOCs or
their surrogate, non-methane organic compounds (NMOCs). The European Union defines VOC
80 as any organic compound having an initial boiling point less than or equal to 250° C measured
at a standard atmospheric pressure of 101.3 kPa (European Union, 1999). The US EPA defines
VOCs as any compound that participates in atmospheric photochemical reactions except for
those that they designate as having minimal reactivity. The term oxygenated VOCs (OVOCs)
(Goldstein and Galbally, 2007; Kwan et al., 2006) has further blurred these definitions, with
85 colloquial usage sometimes being ambiguous as to whether OVOCs are a subset of VOCs or
whether VOCs represent the unoxygenated (i.e., NMHC) suite of compounds. Volatility-based
nomenclature separates VOCs from semi-volatile (SVOC) and intermediate-volatility (IVOC)
species (Robinson et al., 2007). For this study, we use NMOGs, which encompasses all gas-
phase organic compounds (excluding methane), regardless of volatility, degree of oxygenation,
90 or other chemical properties.

While fires emit a significant amount of NMOGs (> 400 Tg yr⁻¹) (Akagi et al., 2011; Yokelson et al., 2008), second only to biogenic sources globally (~1000 Tg yr⁻¹) (Guenther et al., 2012),



95 modeling efforts, particularly at the global scale, have historically represented only a modest
subset of these emissions and their reactivity. This is in part because a large number of reactive
fire NMOGs remain unidentified (Kumar et al., 2018; Hayden et al., 2022; Akagi et al., 2011).
While progress has been made on measuring emissions of many fire NMOGs, these
measurements have not yet been incorporated into models with global coverage. Given the
significant, but insufficiently characterized variability in emission with both fuel and fire
100 characteristics, this challenges integration into fire emission inventories. To represent emitted
species, fire emissions inventories generally apply emission factors (EFs) to estimates of dry
matter (DM) burned. Variation among fire inventories is generally driven by differences in DM,
rather than EFs (Carter et al., 2020); though, NMOG EFs often have greater variability amongst
inventories. Akagi et al. (2011) estimated both species-specific NMOC EFs, as well as the EF for
105 the total of identified + unidentified NMOC mass (for various ecosystems (e.g., for savannas, the
fraction of NMOC emitted mass that is unidentified is ~50% - this number is typical across the
other ecosystems). They also identify unknown NMOCs as one of the largest sources of BB
emissions uncertainties. The GFED version 4 with small fires (GFED4s) inventory (van der Werf
et al., 2017) includes the Akagi et al. (2011) NMOG EFs. The Fire Inventory from NCAR
110 (FINN) v1.5 also uses the Akagi et al. (2011) species-specific EFs as well as total NMOC, and
total non-methane hydrocarbon (NMHC) EFs (Wiedinmyer et al., 2011). Both the Quick Fire
Emissions Dataset (QFED)(Darmenov and daSilva, 2014) and Global Fire Assimilation System
(GFAS)(Kaiser et al., 2012) rely mostly on an older EF compilation (Andreae and Merlet, 2001)
with a few small updates.

115

Several recent scientific advances, including a new fire EF compilation, improved
instrumentation, and fire-focused field campaigns, provide opportunities to enhance our
understanding of NMOGs from fires. Andreae (2019) updated the EFs compiled by Akagi et al.
(2011) and Andreae and Merlet (2001) and added 28 more chemical species, including many fire
120 NMOGs. Recent improvements in instrumentation, especially proton-transfer-reaction time-of-
flight mass spectrometry (PTR-ToF-MS) and gas chromatography (GC), enable high resolution
NMOG measurements, providing the exact molecular formulas and isomer distributions of
detected NMOGs (Hatch et al., 2015; Gilman et al., 2015) and quantification of a substantial
portion of the total carbon mass (Koss et al., 2018). Because OH is generally the dominant



125 oxidant of most fire NMOGs, the inverse of the OH lifetime (or the OH reactivity, OHR) can be
a useful metric to understand the reactivity of fires, where a gap between summed observed OHR
and calculated OHR based on OH lifetimes can point to unidentified NMOGs or oxidation
products (Yang et al., 2016). Lab studies have shown that, from fires, furans, oxygenated
aromatics, and aliphatic hydrocarbons (e.g., monoterpenes) contribute substantially to both
130 calculated and measured OHR and that furans and phenolic compounds are among the most
reactive (Coggon et al., 2019; Hatch et al., 2015). The contribution of fires to global OHR has
not been quantified. Growing interest in the impacts of fires on tropospheric composition has
motivated recent fire campaigns in regions with large and growing fire emissions.

135 These advances suggest that there are opportunities to improve the modeling of NMOGs from
fires and their impacts. In this work, we use the GEOS-Chem chemical transport model (CTM)
and recent lab and field observations to investigate and improve our simulation of fire NMOGs.
We then use this model to characterize the importance of fires to atmospheric reactivity (through
their contribution to total NMOG concentrations and OHR) both globally and regionally.

140

2 Model description

The GEOS-Chem model

We use GEOS-Chem (<https://geos-chem.org>, last access: 15 January 2021), a global CTM, to
explore fire NMOGs globally and in specific large fire regions and outflow regions, such as the
145 US, boreal Canada, the Amazon, and Africa. GEOS-Chem is driven by assimilated meteorology
from the Modern-Era Retrospective analysis for Research and Applications, Version 2
(MERRA-2), from the NASA Global Modeling and Assimilation Office (GMAO). We use
version 13.0.0 (<https://zenodo.org/record/4618180>) of GEOS-Chem with a horizontal resolution
of $2^\circ \times 2.5^\circ$ and 47 vertical levels with a chemical time step of 20 min and a transport time step
150 of 10 min as recommended by Philip et al. (2016). We perform 12-month spin-up simulations
prior to the time periods of interest, June-July 2008, May-June 2012, April-August 2016,
January-December 2017, October 2018, and January-December 2019. We also perform nested
simulations over North America at $0.5^\circ \times 0.625^\circ$ (with boundary conditions from the global



simulation) for comparison against DC3, FIREX-AQ, and ARCTAS observations (see Section 4)
155 with chemistry and transport time steps of 10 and 5 min, respectively.

GEOS-Chem includes $\text{SO}_4^{2-}/\text{NO}_3^-/\text{NH}_4^+$ thermodynamics (Fountoukis and Nenes, 2007)
coupled to an O_3 -VOC- NO_x -oxidant chemical mechanism (Chan Miller et al., 2017; Mao et al.,
2013; Travis et al., 2016) with integrated Cl-Br-I chemistry (Sherwen et al., 2016). We add
160 aromatic oxidation updates (with benzene, toluene, and xylenes (C8 aromatic compounds
including o-, m-, p- xylenes and ethylbenzene) emissions) per Bates et al. (2021) and ethene and
ethyne chemistry updates per Kwon et al., (2021); both were developed in GEOS-Chem, but not
yet implemented in the standard model. These aromatic and ethene/ethyne chemistry updates
modify oxidant levels, particularly NO_3 , which overall decreases NMOG lifetimes. Bates et al.
165 (2021) estimate an annual global mean increase of +22% for NO_3 . In general, species not directly
involved in the new chemistry are modestly impacted by these changes while, for example,
species like glyoxal and glycolaldehyde, which are important products of the ethene/ethyne
chemistry, undergo large increases.

170 Baseline fire emissions are from the Global Fire Emissions Database version 4 with small fires
(GFED4s; (van der Werf et al. 2017)) and are specified on a daily timescale. Additional details
on fire NMOG emissions are provided in Sect. 3. A sensitivity analysis, described in Sect. 4,
uses FINNv1.5. Anthropogenic emissions (including fossil and biofuel sources) follow the year-
specific CEDS global inventory (Hoesly et al., 2018). Trash burning emissions are from
175 Wiedinmyer et al. (2014). Aircraft emissions are from the Aviation Emissions Inventory Code
(AEIC) inventory (Stettler et al. 2011; Simone et al. 2013). Biogenic emissions are calculated
online from the MEGANv2.1 emissions framework (Guenther et al. 2012).

A typical source attribution method in models zeroes out a specific source and differences that
180 simulation from the baseline. This brute force method is ideal for linear systems, but for non-
linear chemistry, large perturbations to emissions will feed back onto the chemistry (and thus
impact lifetimes). For example, zeroing out fire emissions increases OH concentrations because



the OH sink has been decreased, thereby increasing the rate of oxidation of other species, such as from biogenic sources. Such a depression in isoprene concentrations, for example, may then
185 increase or decrease ozone concentrations, depending on the chemical regime. The HTAP modeling experiments, which were focused on O₃, address this issue with 20% emission perturbation sensitivity studies – a number chosen to produce a discernable (larger than numerical noise) and realistic impact while minimizing non-linearities (Huang et al., 2017). To isolate the influence of fires in our model and minimize these nonlinearities, we run emissions
190 sensitivity simulations with 5% more and less fire emissions (0.95 and 1.05 times fire emissions) and scale up the difference to equate to a 100% perturbation. We compare these runs with the more typical noFires brute force simulation in the SI (see Figs. S1, S2, and S3) and show, for example, that the O₃, OH, and isoprene differences are minimized with the emissions sensitivity approach (Fig. S1). We use this fire sensitivity source-attribution approach throughout this study.

195

To translate the concentrations of reactive compounds to calculated OHR (cOHR) at atmospheric ambient conditions, we define cOHR as the sum of the pressure- and temperature-dependent OH rate constant of a species (from the GEOS-Chem mechanism) with its concentration as follows:

$$cOHR (s^{-1}) = k_{OH,CH_4}[CH_4] + k_{OH,CO}[CO] + k_{OH,NO_2}[NO_2] + \sum k_{OH,NMOG_i}[NMOG_i] + \dots (1)$$

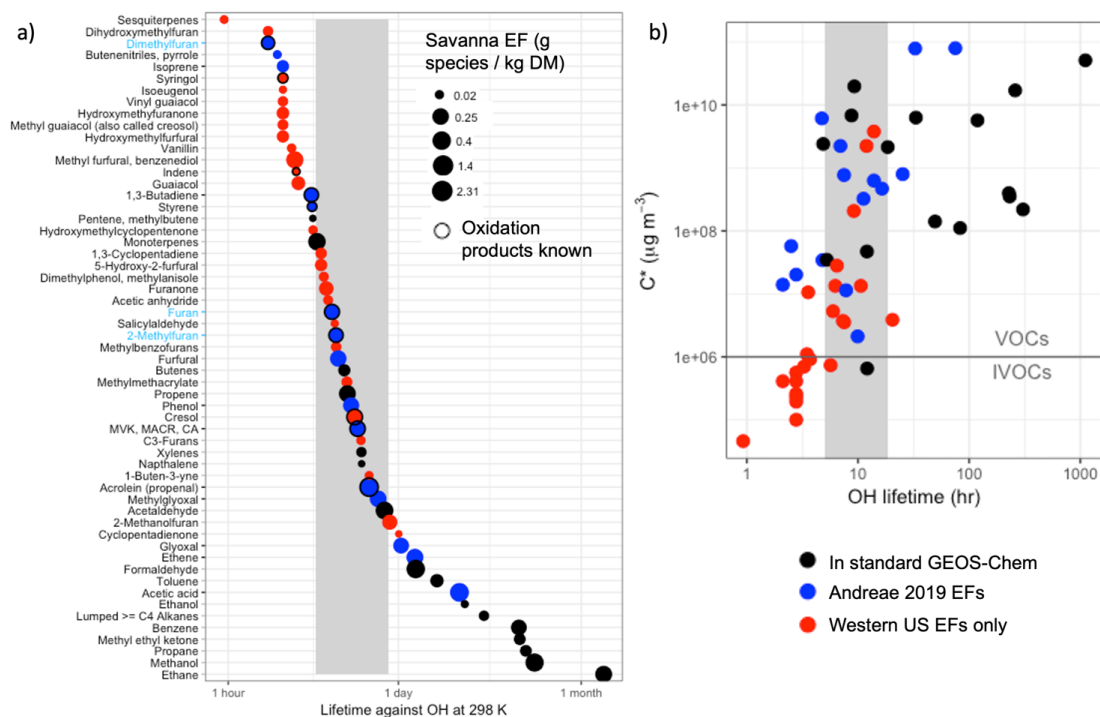
200 where *i* indicates various NMOG species.

3 Updating and expanding fire NMOGs in GEOS-Chem

We update and expand the fire NMOGs in GEOS-Chem by updating existing EFs and then considering additional emissions and chemistry. First, we update our EFs from Akagi et al.
205 (2011) to the newer Andreae (2019) compilation. Total NMOG emissions do not change substantially between the two inventories – in 2019, they decrease by 3.4% from Akagi et al. to Andreae. There is, however, more variation across the different species with, for example, Akagi et al. providing larger savanna EFs for glycoaldehyde (0.25 g/kg DM vs. 0.13 g/kg DM) and glyoxal while Andreae specifies higher values for benzene (0.33 g/kg DM vs. 0.20 g/kg DM),
210 toluene, and xylenes (see Fig. S4 in the SI).



The standard GEOS-Chem model includes fire emissions of 15 NMOG species. The number of possible additional NMOGs from fires is quite large (Akagi et al., 2011). We focus on the feasibility and utility of adding fire NMOGs that Coggon et al. (2019) (building on Koss et al., 215 (2018)) identify as accounting for 95% of fire OHR. We first identify the fire NMOGs already represented in GEOS-Chem (black circles in Fig. 1), then those additional species for which EFs are available from the recently updated compilation by Andreae (2019) in blue, and finally those species for which EFs are only available for western US fuel types as measured during the FIREX lab study (Koss et al., 2018) in red. We size the symbols in Fig. 1a by their EFs for savanna (EFs for other fuel types generally provide a similar relative ranking) to identify the 220 largest NMOG emissions. We order the species in Fig. 1a by their decreasing lifetime against OH with values ranging from 1 hour for sesquiterpenes to over a month for ethane. For context, we provide the same plot by their lifetimes against two other important oxidants, O₃ and NO₃, in the SI (Fig. S5). To explore how chemical lifetimes of these fire NMOGs compare with their 225 physical lifetime in a model grid box, we estimate the approximate lifetime of transport out of a global 2° × 2.5° grid box (~20 hours) and for a nested grid box at 0.5° × 0.625° (~5 hours) using 3 m/s as the surface wind speed (shown as the grey shaded region).



230 Figure 1. (a) NMOGs emitted from fires, shown in descending order of chemical lifetime due to oxidation by OH (at 298 K). Only
the species responsible for 95% of OHR from fires are shown (following Coggon et al., 2019). NMOGs included in the standard
235 GEOS-Chem model are in black, species not included in the standard GEOS-Chem model but where emissions factors are
available in Andreae (2019) are in blue, and species that are only available for western US fuel types from Koss et al. (2018) are
in red. The y-axis tick marks are in black for fire NMOGs added to GEOS-Chem in this study and in blue (with blue labels) when
both the fire NMOG and its oxidation chemistry were added. The points are sized by their relative savanna (labeled “savanna”) emission factor in g species / kg DM burned. The grey vertical box represents an approximate physical
lifetime against transport out of a nested 0.5° × 0.625° grid box (~5 hours) and a 2° × 2.5° grid box (~20 hours). CA stands for
crotonaldehyde. (b) Plot of volatility (C*) against OH lifetime for the species shown in (a) using the same color conventions. The
horizontal line separates VOCs from IVOCs based on their C*.

240 In Fig. 1 most species with chemical lifetimes that exceed the transport timescale out of a model
grid box are already included in the model. Using Andreae (2019) EFs, we add fire emissions of
eight species already included in the model for which fire emissions were previously neglected:
phenol, methyl vinyl ketone (MVK), ethene, isoprene, acetic acid, methylglyoxal, glyoxal, and
lumped aldehydes with three or more carbon atoms, which does not include furfural (RCHO).
245 We also add fire emissions of 1,3-butadiene to the tracer representing alkenes with greater or
equal to three carbons (PRPE). Furans from fires are important for atmospheric reactivity (Koss
et al., 2018; Coggon et al., 2019). We add a new lumped furan tracer, called FURA, that
combines the pyrogenic emissions of furan, 2-methylfuran, and 2,5-dimethylfuran and uses the



OH rate constant of furan ($k_{\text{OH}} = 1.32 \times 10^{-11} \times e^{\frac{-334}{RT}}$) (furan and 2-methylfuran dominate
250 emissions and have very similar lifetimes against OH). In the model, the oxidation of FURA
with OH produces butenedial since that has been shown experimentally with an estimated carbon
balance of 100% C (Bierbach et al., 1995). Thus, we add fire emissions for almost all the species
for which we have Andreae EFs (12 species) to GEOS-Chem. For 2019, these added global fire
emissions (19.6 Tg C) are roughly equivalent to the fire NMOG emissions already in the model
255 (21.8 Tg C) (see Table S1 for species total emissions). The only species with Andreae (2019)
EFs that we do not add to GEOS-Chem are: (1) butenenitriles, which have a very small EF and a
short lifetime against OH, (2) styrene, which also has a chemical lifetime less than the grid box
physical transport time, and (3) furfural. There is a wide spectrum of lesser abundant furans (+
furfural) (Zhao and Wang, 2017) that contribute to furan reactivity; therefore, the representation
260 in this model constitutes a lower bound on furan contributions to total reactivity. We do not
include species where EFs are only available for western US fuel types from Koss et al. (2018).
Figure 1a suggests that nearly all these species are very reactive and short-lived as evidenced by
the red circles being within or below the physical transport time of the grid box.

265 Fig. 1b shows the volatility of these same NMOG species. The species for which we have global
EFs available are almost entirely very volatile and above a commonly held cutoff threshold for
intermediate volatility compounds (IVOCs) versus VOCs ($C^*=1 \times 10^6 \mu\text{g m}^{-3}$ (Ahern et al., 2019
and references therein)). This suggests that both the standard model and our expanded treatment
of NMOGs neglect many NMOG precursors for secondary organic aerosol. This study focuses
270 on the OHR of NMOG from fires; further work is needed to constrain the EFs (Fig 1b. suggests
that global EFs are not available for most IVOCs) and oxidation chemistry of NMOG species
relevant to SOA formation from fires.

Species whose chemical lifetimes are shorter than the physical transport lifetimes (Fig. 1a)
275 contribute strongly to near-field reactivity but are likely not exported from the grid box of
emission. For these species, oxidation rapidly converts emitted species into secondary products,
and it is these products that are exported away from the fire source. However, a detailed
knowledge of the oxidative chemistry of many of these species is lacking (as evidenced by the



small number of black circled species, indicating “oxidation products known” in Fig. 1a). In
280 particular, we note that we do not include several very reactive species (e.g., furfurals, guaiacol)
(Coggon et al., 2019). Hence our model represents a lower limit of reactivity from fires, despite
our inclusion of longer-lived NMOG.

To characterize the amount of carbon mass and reactivity represented in our current model and
285 the potential shortfall in NMOG emissions, we use EFs as proxies for emissions. We first
calculate the total carbon mass based on the sum of the savanna and temperate forest EFs (the
only EFs we have for all species in Fig. 1), and we compare that number to the sum of the
savanna and temperate forest EFs for different subsets (standard GEOS-Chem and updated
GEOS-Chem) of species included in Fig. 1. We note that here and throughout the manuscript,
290 NMOG % values refer to percentage by carbon mass. We find that the standard GEOS-Chem
model represents 49% of the total carbon mass emissions potential of NMOGs suggested in Fig.
1. Our additions to the model increase this to 72%. We then multiply these EFs by the rate
constants with OH at 298 K to represent a proxy for reactivity. From this, we calculate that the
standard model includes 28% of the potential emitted reactivity of savanna and temperate forest
295 fuel type emissions; our model updates add an additional 17% (for a total of 45% of the potential
reactivity). This suggests that the sum of these minor species for which global EFs are not
defined, and therefore that we do not include in our model, contribute over half of the emitted
reactivity from fires. We note that all of these fractions are relative to speciated NMOGs from
Coggon et al. (2019); unspiciated or unidentified NMOG would increase our model shortfall.

300

We use the Andreae (2019) EFs applied to the GFED4s DM and the chemistry updates noted
here for the rest of this analysis unless specifically noted.

4 Exploring observational constraints on fire NMOGs

305 There are limited observational constraints on fire-influenced NMOGs and OHR. We use
observations of OHR made at the Amazon Tall Tower Observatory (ATTO) and of VOCs from



the FIREX and ARCTAS campaigns in addition to measurements of both VOCs and OHR from the Deep Convective Clouds and Chemistry (DC3) campaign. Previous work has shown that the plume-chasing sampling strategy of the WE-CAN 2018 field campaign limits the suitability of this dataset for 3D model evaluation (Carter et al., 2021). While the KORUS-AQ campaign included airborne OHR measurements and some fire influence (median concentration of acetonitrile, a biomass burning tracer (Lobert et al., 1990), ~165 ppt, Fig. S6), the campaign is dominated by anthropogenic sources, which recent work shows may confound the acetonitrile signal (Huangfu et al., 2021); and therefore we do not include this campaign in our analysis. We explore observations of OHR taken during ATom-1 off the coast of western Africa, during which Strode et al. (2018) identified fire influence. However, the aircraft sampled air masses more than 3000 km away from the continental fire source. As a result, most short-lived NMOG have reacted away, and the modeled cOHR is low and dominated by CO (Fig. S7). Thus, ATom-1 is not a good constraint on fire cOHR and the impact of NMOG. There are no other airborne campaigns that we are aware of that have deployed OHR instrumentation in fire-influenced environments.

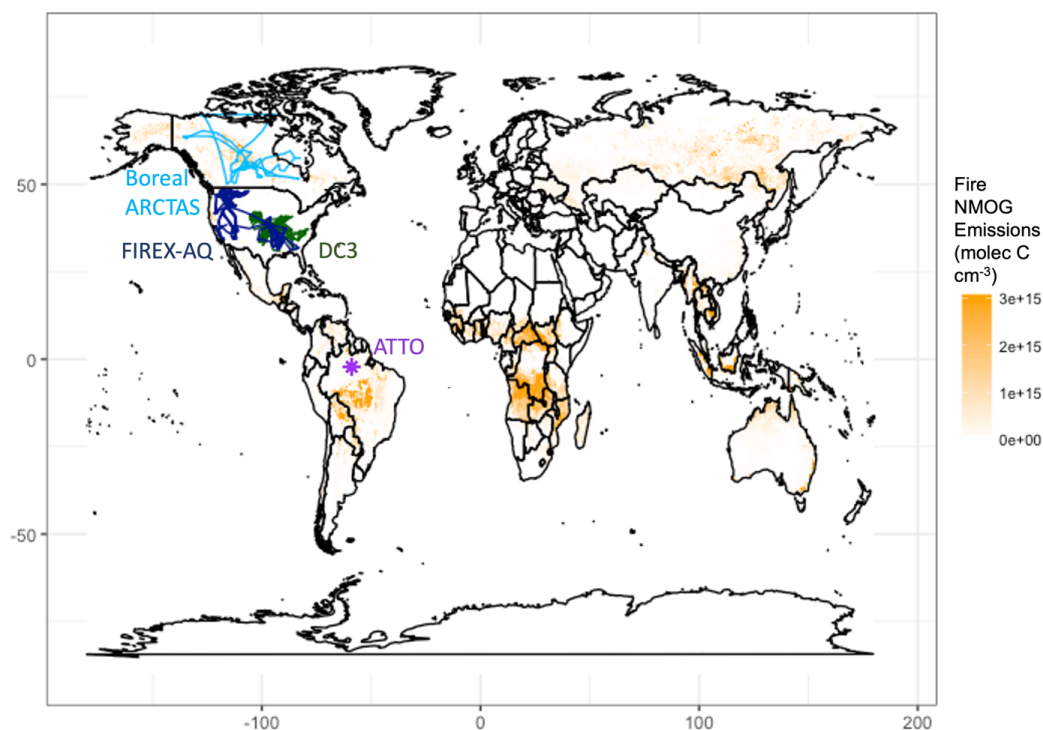




Figure 2. Measurement locations of campaigns used in this analysis overlaid on annual mean NMOG emissions from fires across 1997 – 2019 from GFED4s. Boreal ARCTAS is in light blue, FIREX-AQ in dark blue, DC3 in dark green, and ATTO in purple.

325 We use observations from campaigns that sampled fire-influenced air masses in different regions around the world (Fig. 2). For tower and aircraft campaigns, the model is sampled to the nearest grid box of the measurements both temporally and spatially using the entire 1-min merge of observational data. We then average both the model and the observations to the model grid box.

330 To evaluate our simulation of NMOGs in the US, we explore observations from the NASA DC-8 during the Fire Influence on Regional to Global Environments and Air Quality (FIREX-AQ) campaign, which deployed in the western and eastern US from 15 July through 5 September 2019 with a large suite of NMOG instrumentation aboard. The campaign investigated the chemistry and transport of smoke from both wildfires and prescribed burns in the western and

335 eastern US with flights originating from both Boise, ID, and Salina, KS. CO was measured using a modified commercial off-axis ICOS instrument (Los Gatos Research (LGR) N₂O/CO-30-EP; Baer et al. 2002) at ~ 4.6 μm. Precision was estimated to be 0.4 ppb, and uncertainty for the dry air mole fraction of CO for mixing ratios below 1 ppm to be ± (2.0 ppb + 2%). More details are available from Bourgeois et al. (2022). MVK, furan, 2-methylfuran, and 2,5-dimethylfuran were

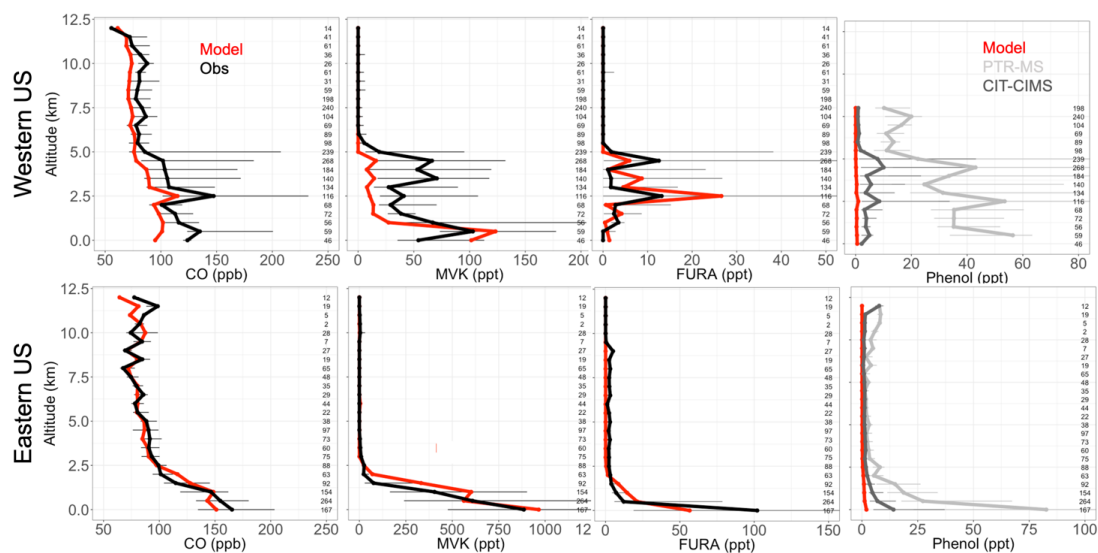
340 measured using the NCAR Trace Organic Gas Analyzer with a Time-of-Flight MS (TOGA-TOF) (Apel et al., 2015; Wang et al., 2021). The TOGA-TOF measurements are reported with a detection limit of 0.5 ppt and an uncertainty (accuracy and precision) of 20%. Phenol was measured using the NOAA PTR Time-of-Flight MS (PTR-ToF-MS) with accuracy of 25% (Müller et al., 2014; de Gouw and Warneke, 2007) and by the California Institute of Technology

345 Chemical Ionization Mass Spectrometer (CIT-CIMS) with an accuracy of 30% (Xu et al., 2021). During the western part of the campaign, the phenol measurements by PTR were affected by a contamination issue above 8 km, so those data have been removed. Generally, the model captures the differing fire influence in the eastern and the western US. For example, in the eastern US, the model captures vertical profiles of CO well (Fig. 3) while in the western US, the

350 model matches the general shape but underestimates the magnitude of the observations and likely the influence of more sporadic fires in the region. Recent papers have also shown that GEOS-Chem struggles to fully capture large wildfires in the western US (e.g., Carter et al., 2021; O'Dell et al., 2019; Zhang et al., 2014) in part because the DM estimates may be underestimated



(Carter et al., 2020) and because GEOS-Chem and other air quality models with a fairly coarse
355 resolution have trouble resolving sub grid processes (Eastham and Jacob, 2017; Rastigejev et al.,
2010), including those involved in fire plumes (Wang et al., 2021; Stockwell et al., 2022).

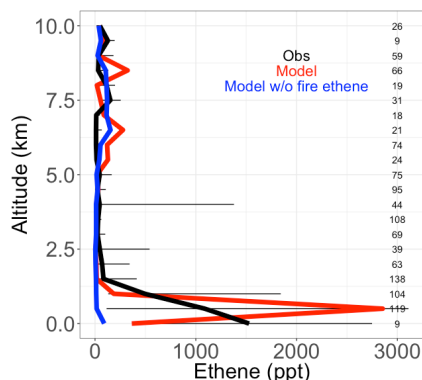


360 *Figure 3. Binned observed (black) and simulated (red) median vertical profiles of CO, MVK, lumped furan species (FURA = furan + 2-methylfuran + 2,5-dimethylfuran), and phenol concentrations from the FIREX-AQ campaign. For phenol, observations using the PTR-MS are in light grey and those from the CIT-CIMS in dark grey. Horizontal bars show the 25th–75th percentile range of measurements in each vertical 0.5-km bin. The number of observations in each bin is shown on the right side of each panel.*

The FIREX-AQ measurements can also be used to evaluate some of our model updates. Figure 3
shows that MVK, an example NMOG for which we added fire emissions in the model, follows
365 similar model performance as CO. We note that more than 80% of simulated MVK during
FIREX-AQ comes from fires. The FIREX-AQ summed observations of the same three furan
species suggest that our new lumped “furan” (FURA) tracer with only fire sources performs well
in the eastern and western US (Fig. 4). This suggests that the furan EFs for US fires like those
sampled are accurately captured in the Andreae (2019) compilation; although they may also be
370 overestimated and thus compensating for an underestimate in the DM burned in GFED4s. Fig. 3
shows that our addition of fire emissions of phenol still underestimates observed concentrations
across all altitudes in the western US and at the surface in the eastern US. Phenol observations
from the CIT-CIMS (dark grey) instrument are a factor of 3 lower than the PTR-MS (light grey).
The model underestimates the lower phenol concentration (CIT-CIMS) by a factor of 8 in the
375 eastern US and 15 in the western US. Given that both instruments were calibrated for phenol, the



380 difference between two measurements is not yet accounted for. The measurements of phenol and other less-studied compounds have substantial uncertainties as indicated by these instrument differences, and more work is needed to understand these uncertainties. However, Taraborrelli et al. (2021) suggest that anthropogenic and fire sources contribute roughly equally to phenol emissions at the global scale. Therefore, both higher phenol emission factors from fires and emissions from anthropogenic sources in the US are likely needed to help resolve the discrepancy seen in Fig 3.



385 Fig 4. Median vertical profiles of binned ethene mixing ratios, including observed (black), simulated (red), and simulated in a sensitivity model run without fire ethene emissions (blue) during the boreal part of the ARCTAS campaign. Horizontal bars show the 25th–75th percentile range of measurements in each vertical 0.5-km bin. The number of observations in each vertical bin is shown on the right side of each panel.

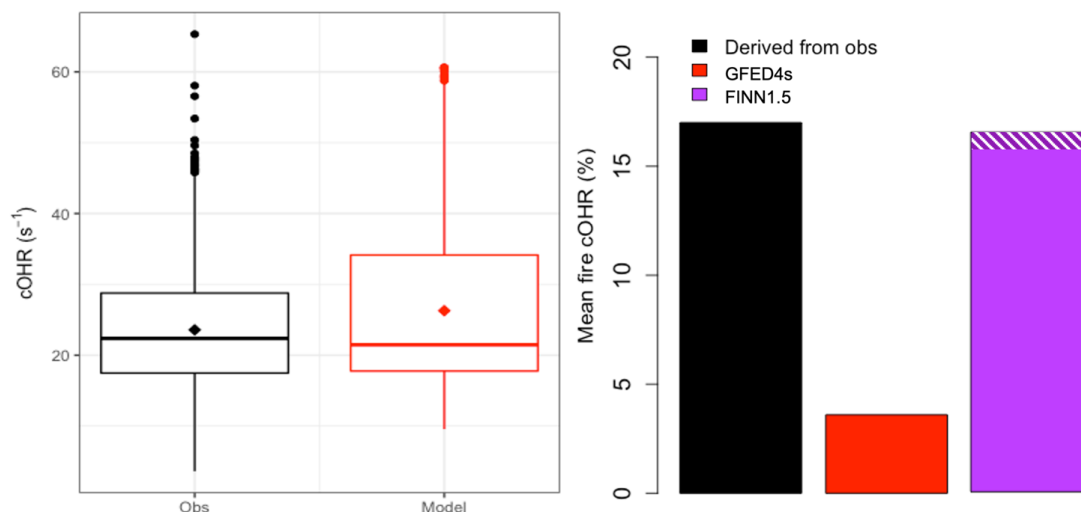
In this study, we add fire emissions of ethene to the model, which may be important in certain regions. We turn to the boreal component of the Arctic Research of the Composition of the Troposphere from Aircraft and Satellites (ARCTAS) campaign to test the fidelity of this addition because the boreal EFs for ethene are high (1.54 g/kg DM, compared to 0.83 g/kg DM for savanna) and there is less anthropogenic influence in the boreal regions to confound a fire-focused model evaluation. The ARCTAS campaign sampled the Arctic region with an emphasis on forest fire smoke plumes using the NASA DC-8 aircraft from 18 June to 13 July 2008 (Jacob et al., 2010). We use observations of ethene from the UC Irvine Whole Air Sampler (WAS). This measurement has a limit of detection of 3 ppt, 3% precision, and 5% accuracy. See Simpson et al. (2011); Colman et al. (2001) for more details. We show that the model (in red), filtered to remove the least fire-influenced points, captures the observed vertical profile of ethene concentrations well, including the large enhancement at the surface (Fig. 4). This is an

390
395



400 improvement over a simulation without fire emissions of ethene (shown in blue), which shows negligible ethene throughout the vertical profile.

Figure 5 compares OHR measurements made at the ATTO site during the fire seasons in October 2018 and September 2019 (Pfannerstill et al., 2021) with the updated GEOS-Chem model
405 simulation. ATTO is situated ~150 km northeast of Manaus, Brazil. We use total OHR measurements taken at 80, 150, and 320m on the tower during two intensive observation periods in October 2018 and September 2019 using the Comparative Reactivity Method (CRM, Sinha et al., 2008), which is described in more detail by Pfannerstill et al., (2021). We confirm that simulated OHR is mostly driven by isoprene during this campaign as Pfannerstill et al. (2021)
410 show for the observations and find that the model (in red; median = 21.5 s^{-1}) captures the overall observed (in black; median = 22.4 s^{-1}) cOHR (Fig. 5a). Pfannerstill et al. (2021) assessed that fires contribute 17% of their OHR measurements (shown in black in Fig. 5b). Our updated simulation with the Andreae (2019) EFs and new chemistry (red in Fig. 5b) underestimates this fire contribution by a factor of ~5. Reddington et al. (2016, 2019) suggested that the FINN1/1.5
415 and GFED3/4s fire inventories underestimate fire emissions by a factor of 2-3 in parts of the Amazon with FINN emissions generally less biased than GFED. Following their analysis, we perform a sensitivity simulation where we use FINN1.5 instead for fire emissions and scale up the emissions to match what was used in the Reddington et al. studies. This simulation (purple) greatly improves model-observations agreement with a mean fire cOHR contribution of 17%
420 (Fig. 5b). Excluding our additions to the NMOG model description (purple and white hatching) does not substantially degrade the agreement with observed OHR from fires, suggesting that underlying biomass burned may be a more important uncertainty in fire NMOG OHR than missing reactive species in this region.



425 *Figure 5. (Left) Boxplots of cOHR during the October 2018 and September 2019 measurement periods at ATTO with*
observations in black and the model in red with medians shown as a horizontal line and means as diamonds. (Right) The mean
percentage contribution from fires during the same time period to cOHR with that derived from observations in black, the model
with GFED4s in red, and a simulation using scaled-up FINN1.5 in purple. The white hatching on the FINN1.5 simulation
indicates the increase in percentage contribution due to of new EFs and chemistry.

430

We also compare observations of NMOGs and OHR during the DC3 campaign, which sampled
in the southeastern and south central US in 18 May – 22 June 2012 (Barth et al., 2015).
Acetonitrile was measured using a PTR-MS (Hansel et al., 1995; Wisthaler et al., 2002). The
OHR measurement is described in detail in Brune et al., (2018); Mao et al., (2009) with a limit of
435 detection for 20s measurements estimated to be $\sim 0.6 \text{ s}^{-1}$. This campaign was influenced by
numerous sources, including fires. Here we explore how well GEOS-Chem captures observed
OHR as a function of fire influence. Figure 6 shows the model skill in reproducing OHR (model
minus observations) against CO and acetonitrile. We find that model skill degrades generally
monotonically with increasing acetonitrile and CO concentrations. No similar trend is observed
440 with anthropogenic tracers such as benzene, suggesting that the model underestimates fire
sources of reactivity. This confirms that we are likely missing emitted fire NMOGs and/or
secondary products during this campaign beyond what we is currently represented in the model,
as suggested in Section 3. Thus, while previous comparisons shown in Section 4 indicate that the
additions we have made to the model have improved our simulation of fire NMOGs, Figure 6
445 confirms further work is needed to fully capture the impact of fires on OH reactivity.

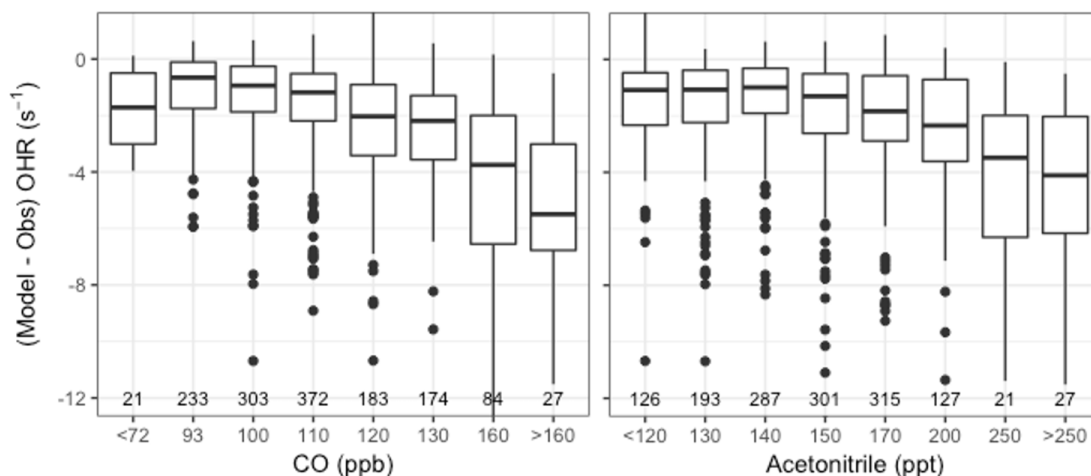
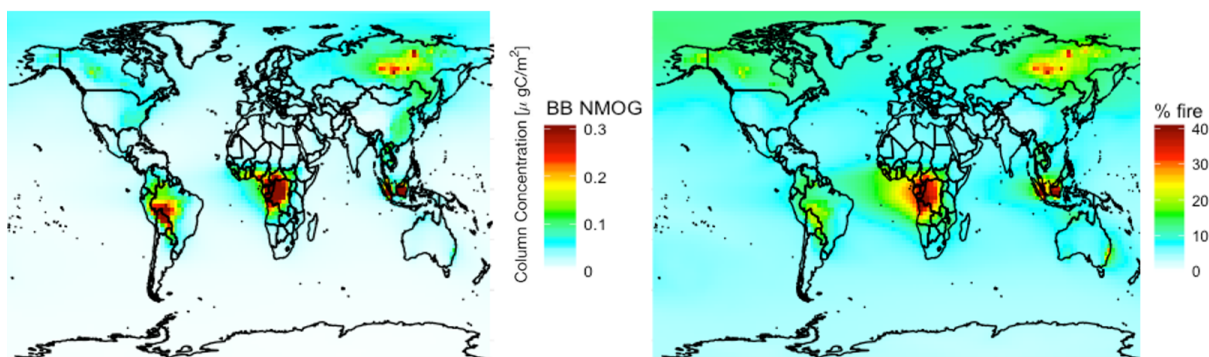


Figure 6. Boxplots of the model minus observed OHR or OHR difference during the DC3 campaign against binned CO (left) and acetonitrile (right) observations. The number of observations in each bin is shown on the bottom of the panel.

450 5 Characterizing fire contribution to global NMOG and atmospheric reactivity

The first estimates of global simulated cOHR highlight the strong gradients in reactivity from source regions to background (Safieddine et al., 2017; Lelieveld et al., 2016). To date, there has been no effort to attribute simulated cOHR to sources. Here we use the source-attribution

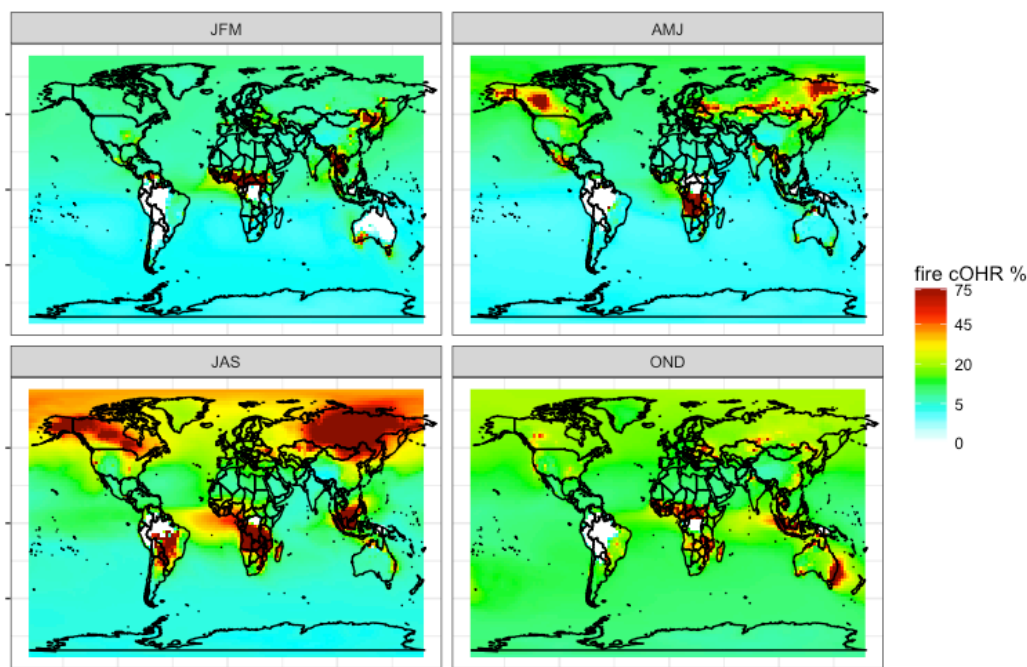
455 approach described in Sect. 2.1 to assess the contribution of fire emissions to global NMOG and cOHR. We note that, given the discussion of Sect. 3, this global simulation should be taken as a lower limit for fire NMOG and cOHR, particularly in fire source regions.





460 *Figure 7. 2019 annual mean simulated (Left) NMOG total column concentrations from fires and (Right) percent contribution of NMOG total column concentrations from fires*

Figure 7 shows simulated annual mean 2019 NMOG total column concentrations and percent contribution from fires. Fires exceed 40% of NMOG annually, not just in the fire seasons, in several fire source regions (e.g., Siberia, central Africa, and Southeast Asia) with elevated levels (~25%) across large parts of the northern hemisphere downwind of sources. Fires also contribute
465 more than 5% of NMOGs nearly everywhere globally, including the remote ocean, driven by RCHO, acetaldehyde, ethene, propene, and DMS.



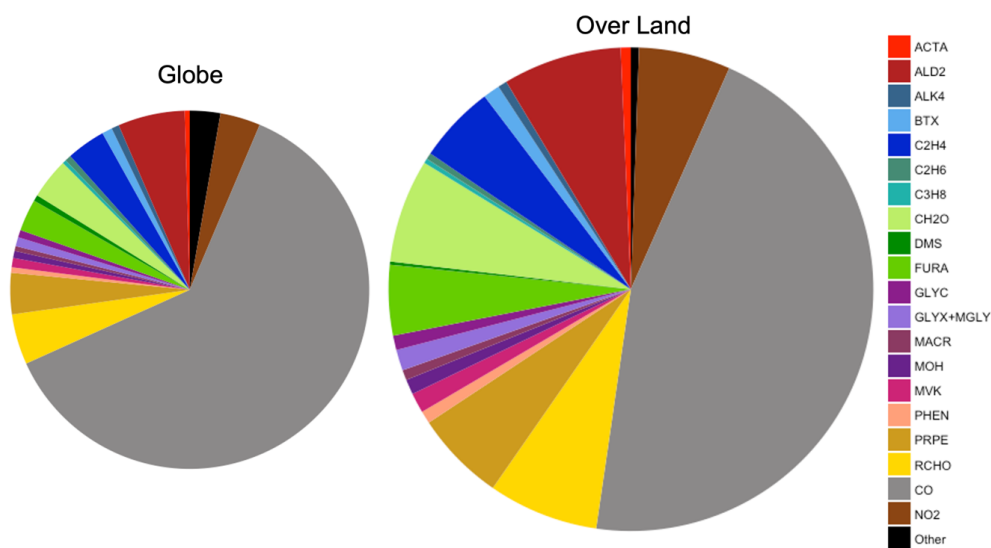
470 *Figure 8. Percent surface cOHR seasonally from fires in 2019 from updated GEOS-Chem simulation (see Sect. 3) using GFED4s DM with Andreae (2019) emission factors. JFM is January, February, March; AMJ is April, May, June; JAS is July, August, September; and OND is October, November, December.*

Figure 8 shows that the contribution of fires to seasonal surface cOHR in 2019 is substantial, exceeding 75% in large fire source regions. The large fire contribution in July, August, September (JAS) and, to a lesser extent, in other seasons, contributes to cOHR beyond the immediate fire emission region. We note that these values are year dependent, and, for example,
475 2019 was a low fire year in the western US where we might expect a larger fire contribution in other years (see Fig. 12 for more discussion of interannual variability). Longer-lived fire species (particularly CO) contribute 10-25% of the background cOHR, peaking in October, November,



and December (OND). Globally in 2019, the annual average simulated fraction of surface reactivity from fires is 15%. The relative export of OH reactivity from a fire source regions is expected to vary with the mix of emissions (i.e. chemical reactivity) and the oxidative environment. This can be explored in fire-dominated regions with strong zonal winds, which produce a clear fire plume. Fig. S8 suggests that the cOHR from fires decays more slowly in plumes from boreal source regions (Canada and Siberia) compared to the tropics (Central Africa), likely reflecting differences in the oxidative loss.

480



485

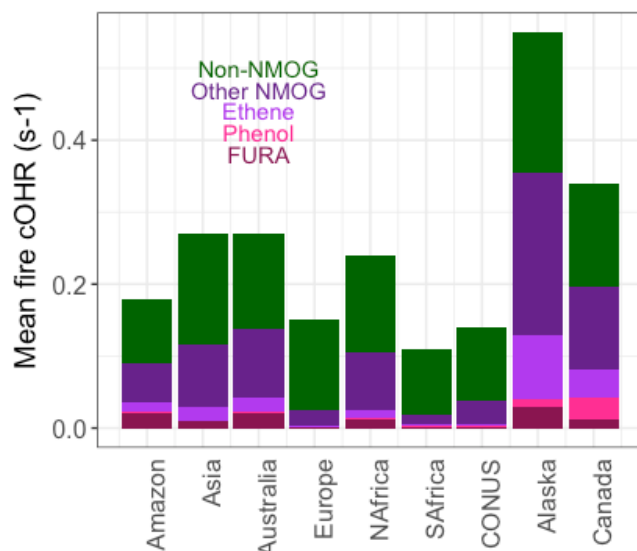
Figure 9. Average global annual mean contribution of chemical species and species groups to simulated surface fire cOHR in 2019 using GFED4s DM for the entire globe and over land only. The two pie charts are approximately sized by their relative fire cOHR (0.16 s^{-1} globally and 0.29 s^{-1} over land). BTX is benzene, toluene, and xylenes. Other ($n=56$) includes species where their annual mean fire cOHR is equal or less than 0.0004, which includes ozone.

490 Figure 9 shows that NMOGs make up 48% of the annual mean surface fire cOHR over land (and 33% over the whole globe), with CO and NO₂ providing the bulk of the remaining cOHR. Of the non-CO annual mean surface fire cOHR, NMOGs make up roughly 90% (colors in Fig. 9). Particularly important NMOG contributors to fire reactivity include acetaldehyde (ALD2 in dark red; 15% of non-CO fire cOHR), formaldehyde (CH₂O in light green; 13% of non-CO fire cOHR), and fire emissions of several NMOG species added in this work – lumped furan (FURA in lime green; 9% of non-CO fire cOHR), ethene (C₂H₄ in royal blue; 10% of non-CO fire cOHR), propene and higher carbon alkenes (PRPE in tan; 11% of non-CO fire cOHR), and

495



lumped aldehydes greater than or equal to three carbons (RCHO in yellow; 14% of non-CO fire cOHR).



500

Figure 10: Mean simulated surface fire cOHR in 2019 using GFED4s DM regionally for the Amazon, Asia, Australia, Europe, northern hemispheric Africa (NAfrica), southern hemispheric Africa (SAfrica), the contiguous US (CONUS), Alaska, and Canada.

Because fires and fuel types differ regionally, Fig. 10 shows the simulated annual mean fire
505 cOHR in several large fire regions. The addition of fire emissions of lumped furans, phenol, and
ethene contribute significantly to fire cOHR depending on region, consistent with their EFs.
Lumped furans, “FURA” (dark red), contribute the most in the Amazon (11%), Australia (7%),
and Alaska (5%) and the least in Europe (1%), southern Africa (2%), and CONUS (2%). The
boreal regions (Alaska and Canada) show larger contributions from phenol (bright pink) (2% and
510 9%, respectively) and ethene (light purple) (16% and 12%, respectively) consistent with high
boreal EFs. Other NMOGs (dark purple) also contribute substantial cOHR in most regions
except Europe, southern Africa, and CONUS where the contribution from CO is dominant. We
note that given our observational analysis for the Amazon (Fig. 5), fire emissions, and thus the
fire cOHR, in this region, and possibly other tropical regions, are likely drastically
515 underestimated in our simulation. We do not adjust regional fire emissions here given that large
uncertainties remain on fire emissions in the Amazon and tropics more generally; therefore, the



values shown in Fig. 10 should certainly be considered a lower estimate (in the Amazon by more than a factor of 3, following Fig. 5).

520

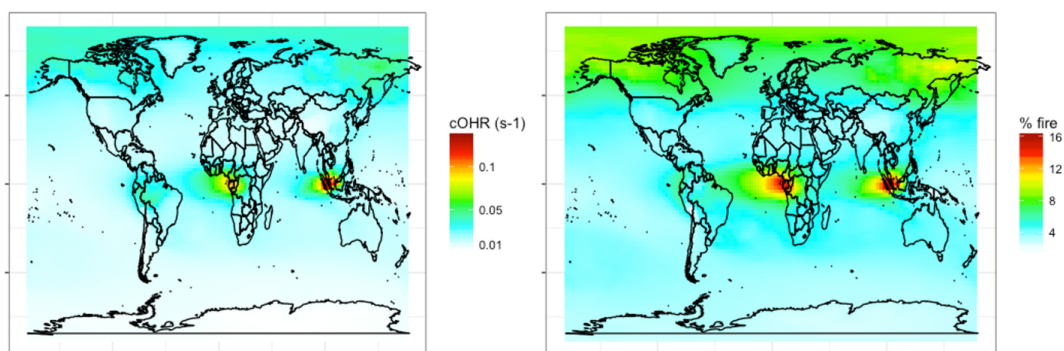
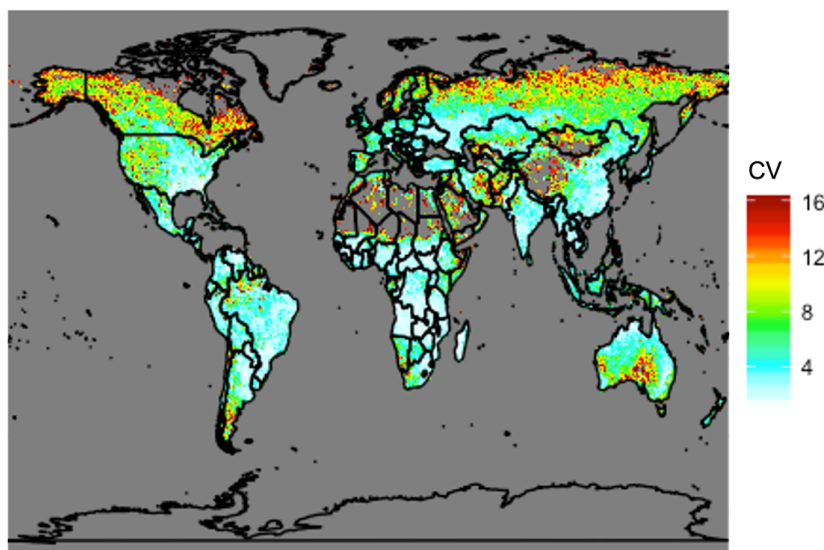


Figure 11: Annual mean simulated (left) fire cOHR and (right) percent of cOHR from fires using GFED4s DM in 2019 at 500 hPa.

NMOGs and associated reactivity in the free troposphere are relevant to the global oxidative capacity, long-range transport, and climate. Figure 11 shows that the simulated contribution of fires in the mid troposphere (500 hPa) to cOHR is 5% globally, but reaches ~15% in the tropics. Fires also contribute more reactivity (~10% annually) in the boreal region. We undertake a similar analysis for 2017 (not shown) where the magnitudes and spatial trends discussed in Figs. 7-11 are similar.

525





530 *Figure 12. Coefficient of variation (CV) of total annual carbon emissions from fires from 1997 to 2019 using GFED4s DM. Coefficient of variation is defined as the standard deviation of a quantity divided by the mean, which is a statistical measure of the relative dispersion of the dataset about the mean.*

The analysis presented above is for a single year (2019). Fire location and magnitudes vary
535 substantially year to year. The global total carbon emissions of NMOGs from the GFED4s
inventory from 1997 to 2019 range from 27 to 48 Tg C yr⁻¹ with 41 Tg C emitted in 2019. This
suggests that our estimates of fire's contribution in the preceding analysis is representative of
average conditions at the global scale but may increase or decrease by roughly a third in different
years. Therefore, across years, the annual global average fraction of surface reactivity due to
540 fires likely ranges from ~10 – 20% with large uncertainties due to the magnitudes of other
anthropogenic and biogenic emissions in any given fire region. To understand interannual
variability at a more local scale, Fig. 12 shows the coefficient of variation, a statistical measure
of the relative dispersion of the data about the mean, for total carbon emissions from fires across
the same years. Given their propensity for large wildfires, the boreal regions, the western US,
545 and Australia show greater year to year variability, which would translate to high variability in
fire contributions to surface cOHR. Conversely, Africa shows very little variation consistent with
human-ignited savanna and agricultural burning each year, suggesting that our single year
estimates of fire contributions to cOHR are generally robust in this region.

550 6 Conclusions

Recent work has suggested that NMOGs from fires may be a large source but noted that we did
not yet have a framework in our models to fully characterize them and their reactivity (Akagi et
al., 2011). Our work provides a first estimate of fire NMOGs globally and regionally and their
contribution to reactivity. We updated fire NMOG EFs to Andreae (2019) from Akagi et al.
555 (2011). We also expanded the model representation by adding new fire NMOGs (e.g., lumped
furans, phenol, ethene), prioritized for their reactivity using data from the FIREX lab studies and
their chemistry. We used a suite of recent observations from the lab (FIREX) to towers (ATTO)
to aircraft campaigns (FIREX-AQ, ARCTAS, DC3) to constrain and test our model
representation. We show that observations support the additions made to the model.



560

Our model suggests that fires are a major contributor to NMOG concentrations, especially near fire source regions and downwind of them. We show that fires provide more than 75% of cOHR in large parts of the northern hemisphere and that fires contribute to a high background (~25%) reactivity beyond their source regions, mostly driven by CO and other long-lived species. We also show that 90% of non-CO annual surface OHR is from NMOGs and that FURA (furan, 2-methylfuran, and 2,5-dimethylfuran) and ethene are important globally for reactivity with phenol more important at a local level in the boreal regions. To our knowledge, this is the first quantification and characterization of the impact and importance of fire for atmospheric reactivity and the first representation of both lumped furans and phenol from fires in GEOS-Chem. However, our analysis is almost certainly a lower limit on the magnitude of reactivity from fire NMOGs because we do not comprehensively include all species emitted from fires, given that for many of these their global EFs and product formation are not well understood. To further improve the representation of fire NMOGs in models, more measurements of speciated NMOG and total OHR are needed to help constrain both the total emissions and reactivity of NMOGs, particularly during field campaigns with fire influence. Further development of oxidative chemical mechanisms for highly reactive NMOGs are also needed to ensure that models better capture the exported reactivity from fires. Finally, while we substantially increase the mass and reactivity from fire NMOGs represented in our model, more work is needed to constrain low-volatility NMOGs that are precursors to SOA.

580

As fires become more intense in the western US and in other temperate and boreal regions due to climate change (e.g., Westerling, 2016; Westerling et al., 2006; Abatzoglou and Williams, 2016; Senande-Rivera et al., 2022) and human forcing leads to different burned area trends globally (Andela et al., 2017), it is becoming ever more important to improve our understanding of fire emissions, their reactivity, and their impact globally. Our work shows that NMOGs from fires contribute substantially to atmospheric reactivity, both locally and globally, highlighting the urgent need to further constrain the sources and transformations of these species.

585

Data availability



590 The GEOS-Chem model is publicly available at: <https://zenodo.org/record/4618180> (GEOS-Chem,
2021). The DC3 campaign data are available at [https://www.
eol.ucar.edu/field_projects/dc3](https://www.eol.ucar.edu/field_projects/dc3) (last access: February 18, 2018), and the ARCTAS campaign data are
available at: <https://www-air.larc.nasa.gov/cgi-bin/ArcView/arctas> (last access: February 18, 2018).
595 ATTO data are available at <https://attodata.org/> (last access: June 4, 2021). FIREX-AQ data are
available at <https://www-air.larc.nasa.gov/cgi-bin/ArcView/firexaq> (last access: April 16, 2022).

Supplement

See SI at [link added by ACP]

600 Author contribution

CLH and TSC formulated the research question and wrote the paper with input from JHK.
TSC performed the modeling and analysis. ECA, DB, MC, AE, GG, RSH, FP, JP, EYP, NGR,
AR, CW, AW, JW, and LX measured CO, VOCs, and OHR during ARCTAS, FIREX-AQ, and
ATTO and provided input on the manuscript.

605

Competing interests

The authors declare that they have no conflict of interest.

Acknowledgements

610 We thank Kelvin Bates for advice on implementing the aromatic hydrocarbon updates and
ethene/ethyne chemistry that were not yet available in the standard GEOS-Chem model. We
also thank Mat Evans for discussing source attribution approaches. We acknowledge Tom
Ryerson for making measurements of CO during FIREX-AQ and William Brune for OHR
measurements and Teresa Campos for CO measurements during DC3.

615

Financial Support

This work was supported by the U.S. National Science Foundation (NSF AGS 1936642). This
material is based upon work supported by the National Center for Atmospheric Research, which
is a major facility sponsored by the National Science Foundation under Cooperative Agreement
620 No. 1852977. ECA and RSH were also funded in part by NASA Award No. 80NSSC18K0633.
JP was supported by the NOAA Cooperative Agreement with CIRES, NA17OAR4320101. The
University of Innsbruck PTR-MS measurements were supported by the Austrian Federal
Ministry for Transport, Innovation and Technology (bmvit, FFG, ASAP).

625 References

Abatzoglou, J. T. and Williams, A. P.: Impact of anthropogenic climate change on wildfire
across western US forests, *Proc Natl Acad Sci USA*, 113, 11770–11775,
<https://doi.org/10.1073/pnas.1607171113>, 2016.



- 630 Ahern, A. T., Robinson, E. S., Tkacik, D. S., Saleh, R., Hatch, L. E., Barsanti, K. C., Stockwell, C. E., Yokelson, R. J., Presto, A. A., Robinson, A. L., Sullivan, R. C., and Donahue, N. M.: Production of Secondary Organic Aerosol During Aging of Biomass Burning Smoke From Fresh Fuels and Its Relationship to VOC Precursors, 124, 3583–3606, <https://doi.org/10.1029/2018JD029068>, 2019.
- 635 Akagi, S., Yokelson, R., Wiedinmyer, C., Alvarado, M., Reid, J., Karl, T., Crouse, J., and Wennberg, P.: Emission Factors for Open and Domestic Biomass Burning for Use in Atmospheric Models, 4039–4072, 2011.
- 640 Andela, N., Morton, D. C., Giglio, L., Chen, Y., Werf, G. R. van der, Kasibhatla, P. S., DeFries, R. S., Collatz, G. J., Hantson, S., Kloster, S., Bachelet, D., Forrest, M., Lasslop, G., Li, F., Mangeon, S., Melton, J. R., Yue, C., and Randerson, J. T.: A human-driven decline in global burned area, 356, 1356–1362, <https://doi.org/10.1126/science.aal4108>, 2017.
- Andreae, M. O.: Emission of trace gases and aerosols from biomass burning – an updated assessment, 19, 8523–8546, <https://doi.org/10.5194/acp-19-8523-2019>, 2019.
- Andreae, M. O. and Merlet, P.: Emission of trace gases and aerosols from biomass burning, 15, 955–966, <https://doi.org/10.1029/2000GB001382>, 2001.
- 645 Apel, E. C., Hornbrook, R. S., Hills, A. J., Blake, N. J., Barth, M. C., Weinheimer, A., Cantrell, C., Rutledge, S. A., Basarab, B., Crawford, J., Diskin, G., Homeyer, C. R., Campos, T., Flocke, F., Fried, A., Blake, D. R., Brune, W., Pollack, I., Peischl, J., Ryerson, T., Wennberg, P. O., Crouse, J. D., Wisthaler, A., Mikoviny, T., Huey, G., Heikes, B., O’Sullivan, D., and Riemer, D. D.: Upper tropospheric ozone production from lightning NO_x-impacted convection: Smoke ingestion case study from the DC3 campaign, 120, 2505–2523, <https://doi.org/10.1002/2014JD022121>, 2015.
- 650 Baer, D. S., Paul, J. B., Gupta, M., and O’Keefe, A.: Sensitive absorption measurements in the near-infrared region using off-axis integrated-cavity-output spectroscopy, *Appl Phys B*, 75, 261–265, <https://doi.org/10.1007/s00340-002-0971-z>, 2002.
- 655 Barth, M. C., Cantrell, C. A., Brune, W. H., Rutledge, S. A., Crawford, J. H., Huntrieser, H., Carey, L. D., MacGorman, D., Weisman, M., Pickering, K. E., Bruning, E., Anderson, B., Apel, E., Biggerstaff, M., Campos, T., Campuzano-Jost, P., Cohen, R., Crouse, J., Day, D. A., Diskin, G., Flocke, F., Fried, A., Garland, C., Heikes, B., Honomichl, S., Hornbrook, R., Huey, L. G., Jimenez, J. L., Lang, T., Lichtenstern, M., Mikoviny, T., Nault, B., O’Sullivan, D., Pan, L. L., 660 Peischl, J., Pollack, I., Richter, D., Riemer, D., Ryerson, T., Schlager, H., St. Clair, J., Walega, J., Weibring, P., Weinheimer, A., Wennberg, P., Wisthaler, A., Wooldridge, P. J., and Ziegler, C.: The Deep Convective Clouds and Chemistry (DC3) Field Campaign, *Bull. Amer. Meteor. Soc.*, 96, 1281–1309, <https://doi.org/10.1175/BAMS-D-13-00290.1>, 2015.
- 665 Bates, K. H., Jacob, D. J., Li, K., Ivatt, P. D., Evans, M. J., Yan, Y., and Lin, J.: Development and evaluation of a new compact mechanism for aromatic oxidation in atmospheric models, *Atmos. Chem. Phys.*, 21, 18351–18374, <https://doi.org/10.5194/acp-21-18351-2021>, 2021.



- Bernath, P., Boone, C., and Crouse, J.: Wildfire smoke destroys stratospheric ozone, 375, 1292–1295, <https://doi.org/10.1126/science.abm5611>, 2022.
- 670 Bierbach, A., Barnes, I., and Becker, K. H.: Product and kinetic study of the oh-initiated gas-phase oxidation of Furan, 2-methylfuran and furanaldehydes at ≈ 300 K, *Atmospheric Environment*, 29, 2651–2660, [https://doi.org/10.1016/1352-2310\(95\)00096-H](https://doi.org/10.1016/1352-2310(95)00096-H), 1995.
- 675 Bourgeois, I., Peischl, J., Neuman, J. A., Brown, S. S., Thompson, C. R., Aikin, K. C., Allen, H. M., Angot, H., Apel, E. C., Baublitz, C. B., Brewer, J. F., Campuzano-Jost, P., Commane, R., Crouse, J. D., Daube, B. C., DiGangi, J. P., Diskin, G. S., Emmons, L. K., Fiore, A. M., Gkatzelis, G. I., Hills, A., Hornbrook, R. S., Huey, L. G., Jimenez, J. L., Kim, M., Lacey, F., McKain, K., Murray, L. T., Nault, B. A., Parrish, D. D., Ray, E., Sweeney, C., Tanner, D., Wofsy, S. C., and Ryerson, T. B.: Large contribution of biomass burning emissions to ozone throughout the global remote troposphere, *PNAS*, 118, <https://doi.org/10.1073/pnas.2109628118>, 2021.
- 680 Bourgeois, I., Peischl, J., Neuman, J. A., Brown, S. S., Allen, H. M., Campuzano-Jost, P., Coggon, M. M., DiGangi, J. P., Diskin, G. S., Gilman, J. B., Gkatzelis, G. I., Guo, H., Halliday, H., Hanisco, T. F., Holmes, C. D., Huey, L. G., Jimenez, J. L., Lamplugh, A. D., Lee, Y. R., Lindaas, J., Moore, R. H., Nowak, J. B., Pagonis, D., Rickly, P. S., Robinson, M. A., Rollins, A. W., Selimovic, V., St. Clair, J. M., Tanner, D., Vasquez, K. T., Veres, P. R., Warneke, C.,
685 Wennberg, P. O., Washenfelder, R. A., Wiggins, E. B., Womack, C. C., Xu, L., Zarzana, K. J., and Ryerson, T. B.: Comparison of airborne measurements of NO, NO₂, HONO, NO_y and CO during FIREX-AQ, *Gases/In Situ Measurement/Instruments and Platforms*, <https://doi.org/10.5194/amt-2021-432>, 2022.
- 690 Brune, W. H., Ren, X., Zhang, L., Mao, J., Miller, D. O., Anderson, B. E., Blake, D. R., Cohen, R. C., Diskin, G. S., Hall, S. R., Hanisco, T. F., Huey, L. G., Nault, B. A., Peischl, J., Pollack, I., Ryerson, T. B., Shingler, T., Sorooshian, A., Ullmann, K., Wisthaler, A., and Wooldridge, P. J.: Atmospheric oxidation in the presence of clouds during the Deep Convective Clouds and
695 Chemistry (DC3) study, *Atmos. Chem. Phys.*, 18, 14493–14510, <https://doi.org/10.5194/acp-18-14493-2018>, 2018.
- Carter, T. S., Heald, C. L., Jimenez, J. L., Campuzano-Jost, P., Kondo, Y., Moteki, N., Schwarz, J. P., Wiedinmyer, C., Darmenov, A. S., da Silva, A. M., and Kaiser, J. W.: How emissions uncertainty influences the distribution and radiative impacts of smoke from fires in North
700 America, *Atmospheric Chemistry & Physics*, 20, 2073–2097, <https://doi.org/10.5194/acp-20-2073-2020>, 2020.
- 705 Carter, T. S., Heald, C. L., Cappa, C. D., Kroll, J. H., Campos, T. L., Coe, H., Cotterell, M. I., Davies, N. W., Farmer, D. K., Fox, C., Garofalo, L. A., Hu, L., Langridge, J. M., Levin, E. J. T., Murphy, S. M., Pokhrel, R. P., Shen, Y., Szpek, K., Taylor, J. W., and Wu, H.: Investigating Carbonaceous Aerosol and Its Absorption Properties From Fires in the Western United States (WE-CAN) and Southern Africa (ORACLES and CLARIFY), 126, e2021JD034984, <https://doi.org/10.1029/2021JD034984>, 2021.



- Chan Miller, C., Jacob, D. J., Marais, E. A., Yu, K., Travis, K. R., Kim, P. S., Fisher, J. A., Zhu, L., Wolfe, G. M., Hanisco, T. F., Keutsch, F. N., Kaiser, J., Min, K.-E., Brown, S. S., Washenfelder, R. A., González Abad, G., and Chance, K.: Glyoxal yield from isoprene oxidation and relation to formaldehyde: chemical mechanism, constraints from SENEX aircraft observations, and interpretation of OMI satellite data, *17*, 8725–8738, <https://doi.org/10.5194/acp-17-8725-2017>, 2017.
- Coggon, M. M., Lim, C. Y., Koss, A. R., Sekimoto, K., Yuan, B., Gilman, J. B., Hagan, D. H., Selimovic, V., Zarzana, K. J., Brown, S. S., Roberts, J. M., Müller, M., Yokelson, R., Wisthaler, A., Krechmer, J. E., Jimenez, J. L., Cappa, C., Kroll, J. H., de Gouw, J., and Warneke, C.: OH chemistry of non-methane organic gases (NMOGs) emitted from laboratory and ambient biomass burning smoke: evaluating the influence of furans and oxygenated aromatics on ozone and secondary NMOG formation, *Atmos. Chem. Phys.*, *19*, 14875–14899, <https://doi.org/10.5194/acp-19-14875-2019>, 2019.
- Colman, J. J., Swanson, A. L., Meinardi, S., Sive, B. C., Blake, D. R., and Rowland, F. S.: Description of the Analysis of a Wide Range of Volatile Organic Compounds in Whole Air Samples Collected during PEM-Tropics A and B, *Anal. Chem.*, *73*, 3723–3731, <https://doi.org/10.1021/ac010027g>, 2001.
- The Quick Fire Emissions Dataset (QFED) – Documentation of versions 2.1, 2.2 and 2.4, NASA Technical Report Series on Global Modeling and Data Assimilation, NASA TM-2013-104606: [https://scholar.google.com/scholar?lookup=0&q=The+Quick+Fire+Emissions+Dataset+\(QFED\):+Documentation+of+versions+2.1,+2.2+and+2.4.%22+NASA+Technical+Report+Series+on+G+lobal+Modeling+and+Data+Assimilation&hl=en&as_sdt=0,22](https://scholar.google.com/scholar?lookup=0&q=The+Quick+Fire+Emissions+Dataset+(QFED):+Documentation+of+versions+2.1,+2.2+and+2.4.%22+NASA+Technical+Report+Series+on+G+lobal+Modeling+and+Data+Assimilation&hl=en&as_sdt=0,22), last access: 16 June 2020.
- Eastham, S. D. and Jacob, D. J.: Limits on the ability of global Eulerian models to resolve intercontinental transport of chemical plumes, *Atmos. Chem. Phys.*, *17*, 2543–2553, <https://doi.org/10.5194/acp-17-2543-2017>, 2017.
- European Union: Council Directive 1999/13/EC of 11 March 1999 on the limitation of emissions of volatile organic compounds due to the use of organic solvents in certain activities and installations, OJ L, 085, 1999.
- Fountoukis, C. and Nenes, A.: ISORROPIA II: a computationally efficient thermodynamic equilibrium model for K^+ , Ca^{2+} , Mg^{2+} , NH_4^+ , Na^+ , SO_4^{2-} , NO_3^- , Cl^- , H_2O aerosols, *48*, 2007.
- Gilman, J. B., Lerner, B. M., Kuster, W. C., Goldan, P. D., Warneke, C., Veres, P. R., Roberts, J. M., de Gouw, J. A., Burling, I. R., and Yokelson, R. J.: Biomass burning emissions and potential air quality impacts of volatile organic compounds and other trace gases from fuels common in the US, *15*, 13915–13938, <https://doi.org/10.5194/acp-15-13915-2015>, 2015.
- Goldstein, A. H. and Galbally, I. E.: in the Earth's Atmosphere, *8*, 2007.
- de Gouw, J. and Warneke, C.: Measurements of volatile organic compounds in the earth's atmosphere using proton-transfer-reaction mass spectrometry, *Mass Spectrom Rev*, *26*, 223–257, <https://doi.org/10.1002/mas.20119>, 2007.



- Guenther, A. B., Jiang, X., Heald, C. L., Sakulyanontvittaya, T., Duhl, T., Emmons, L. K., and Wang, X.: The Model of Emissions of Gases and Aerosols from Nature version 2.1 (MEGAN2.1): an extended and updated framework for modeling biogenic emissions, 5, 1471–1492, <https://doi.org/10.5194/gmd-5-1471-2012>, 2012.
- 750 Hansel, A., Jordan, A., Holzinger, R., Prazeller, P., Vogel, W., and Lindinger, W.: Proton transfer reaction mass spectrometry: on-line trace gas analysis at the ppb level, *International Journal of Mass Spectrometry and Ion Processes*, 149–150, 609–619, [https://doi.org/10.1016/0168-1176\(95\)04294-U](https://doi.org/10.1016/0168-1176(95)04294-U), 1995.
- 755 Hatch, L. E., Luo, W., Pankow, J. F., Yokelson, R. J., Stockwell, C. E., and Barsanti, K. C.: Identification and quantification of gaseous organic compounds emitted from biomass burning using two-dimensional gas chromatography–time-of-flight mass spectrometry, 15, 1865–1899, <https://doi.org/10.5194/acp-15-1865-2015>, 2015.
- 760 Hayden, K., Li, S.-M., Liggio, J., Wheeler, M., Wentzell, J., Leithead, A., Brickell, P., Mittermeier, R., Oldham, Z., Mihele, C., Staebler, R., Moussa, S., Darlington, A., Steffen, A., Wolde, M., Thompson, D., Chen, J., Griffin, D., Eckert, E., Ditto, J., He, M., and Gentner, D.: Reconciling the total carbon budget for boreal forest wildfire emissions using airborne observations, 1–62, <https://doi.org/10.5194/acp-2022-245>, 2022.
- 765 Hobbs, P. V., Sinha, P., Yokelson, R. J., Christian, T. J., Blake, D. R., Gao, S., Kirchstetter, T. W., Novakov, T., and Pilewskie, P.: Evolution of gases and particles from a savanna fire in South Africa, 108, <https://doi.org/10.1029/2002JD002352>, 2003.
- 770 Hoesly, R. M., Smith, S. J., Feng, L., Klimont, Z., Janssens-Maenhout, G., Pitkanen, T., Seibert, J. J., Vu, L., Andres, R. J., Bolt, R. M., Bond, T. C., Dawidowski, L., Kholod, N., Kurokawa, J., Li, M., Liu, L., Lu, Z., Moura, M. C. P., O'Rourke, P. R., and Zhang, Q.: Historical (1750–2014) anthropogenic emissions of reactive gases and aerosols from the Community Emissions Data System (CEDS), 11, 369–408, <https://doi.org/10.5194/gmd-11-369-2018>, 2018.
- 775 Huang, M., Carmichael, G. R., Pierce, R. B., Jo, D. S., Park, R. J., Flemming, J., Emmons, L. K., Bowman, K. W., Henze, D. K., Davila, Y., Sudo, K., Jonson, J. E., Tronstad Lund, M., Janssens-Maenhout, G., Dentener, F. J., Keating, T. J., Oetjen, H., and Payne, V. H.: Impact of intercontinental pollution transport on North American ozone air pollution: an HTAP phase 2 multi-model study, *Atmos. Chem. Phys.*, 17, 5721–5750, <https://doi.org/10.5194/acp-17-5721-2017>, 2017.
- 780 Huangfu, Y., Yuan, B., Wang, S., Wu, C., He, X., Qi, J., de Gouw, J., Warneke, C., Gilman, J. B., Wisthaler, A., Karl, T., Graus, M., Jobson, B. T., and Shao, M.: Revisiting Acetonitrile as Tracer of Biomass Burning in Anthropogenic-Influenced Environments, 48, e2020GL092322, <https://doi.org/10.1029/2020GL092322>, 2021.
- 785 Jacob, D. J., Crawford, J. H., Maring, H., Clarke, A. D., Dibb, J. E., Emmons, L. K., Ferrare, R. A., Hostetler, C. A., Russell, P. B., Singh, H. B., Thompson, A. M., Shaw, G. E., McCauley, E., Pederson, J. R., and Fisher, J. A.: The Arctic Research of the Composition of the Troposphere from Aircraft and Satellites (ARCTAS) mission: design, execution, and first results, *Atmos. Chem. Phys.*, 10, 5191–5212, <https://doi.org/10.5194/acp-10-5191-2010>, 2010.



- Jaffe, D., Chand, D., Hafner, W., Westerling, A., and Spracklen, D.: Influence of Fires on O₃ Concentrations in the Western U.S., *Environ. Sci. Technol.*, 42, 5885–5891, <https://doi.org/10.1021/es800084k>, 2008.
- 790 Jaffe, D. A., Wigder, N., Downey, N., Pfister, G., Boynard, A., and Reid, S. B.: Impact of Wildfires on Ozone Exceptional Events in the Western U.S., *Environ. Sci. Technol.*, 47, 11065–11072, <https://doi.org/10.1021/es402164f>, 2013.
- 795 Jaffe, D. A., Cooper, O. R., Fiore, A. M., Henderson, B. H., Tonnesen, G. S., Russell, A. G., Henze, D. K., Langford, A. O., Lin, M., and Moore, T.: Scientific assessment of background ozone over the U.S.: Implications for air quality management, *Elementa: Science of the Anthropocene*, 6, 56, <https://doi.org/10.1525/elementa.309>, 2018.
- Kaiser, J. W., Heil, A., Andreae, M. O., Benedetti, A., Chubarova, N., Jones, L., Morcrette, J.-J., Razinger, M., Schultz, M. G., Suttie, M., and van der Werf, G. R.: Biomass burning emissions estimated with a global fire assimilation system based on observed fire radiative power, *Biogeosciences*, 9, 527–554, <https://doi.org/10.5194/bg-9-527-2012>, 2012.
- 800 Koss, A. R., Sekimoto, K., Gilman, J. B., Selimovic, V., Coggon, M. M., Zarzana, K. J., Yuan, B., Lerner, B. M., Brown, S. S., Jimenez, J. L., Krechmer, J., Roberts, J. M., Warneke, C., Yokelson, R. J., and Gouw, J. de: Non-methane organic gas emissions from biomass burning: identification, quantification, and emission factors from PTR-ToF during the FIREX 2016 laboratory experiment, 18, 3299–3319, <https://doi.org/10.5194/acp-18-3299-2018>, 2018.
- 805 Kumar, V., Chandra, B. P., and Sinha, V.: Large unexplained suite of chemically reactive compounds present in ambient air due to biomass fires, *Sci Rep*, 8, 626, <https://doi.org/10.1038/s41598-017-19139-3>, 2018.
- 810 Kwan, A. J., Crounse, J. D., Clarke, A. D., Shinzuka, Y., Anderson, B. E., Crawford, J. H., Avery, M. A., McNaughton, C. S., Brune, W. H., Singh, H. B., and Wennberg, P. O.: On the flux of oxygenated volatile organic compounds from organic aerosol oxidation, 33, <https://doi.org/10.1029/2006GL026144>, 2006.
- 815 Kwon, H.-A., Park, R. J., Oak, Y. J., Nowlan, C. R., Janz, S. J., Kowalewski, M. G., Fried, A., Walega, J., Bates, K. H., Choi, J., Blake, D. R., Wisthaler, A., and Woo, J.-H.: Top-down estimates of anthropogenic VOC emissions in South Korea using formaldehyde vertical column densities from aircraft during the KORUS-AQ campaign, *Elementa: Science of the Anthropocene*, 9, 00109, <https://doi.org/10.1525/elementa.2021.00109>, 2021.
- Lelieveld, J., Gromov, S., Pozzer, A., and Taraborrelli, D.: Global tropospheric hydroxyl distribution, budget and reactivity, 16, 12477–12493, <https://doi.org/10.5194/acp-16-12477-2016>, 2016.
- 820 Lobert, J. M., Scharffe, D. H., Hao, W. M., and Crutzen, P. J.: Importance of biomass burning in the atmospheric budgets of nitrogen-containing gases, *Nature*, 346, 552–554, <https://doi.org/10.1038/346552a0>, 1990.



- 825 Mao, J., Ren, X., Brune, W. H., Olson, J. R., Crawford, J. H., Fried, A., Huey, L. G., Cohen, R. C., Heikes, B., Singh, H. B., Blake, D. R., Sachse, G. W., Diskin, G. S., Hall, S. R., and Shetter, R. E.: Airborne measurement of OH reactivity during INTEX-B, 11, 2009.
- Mao, J., Paulot, F., Jacob, D. J., Cohen, R. C., Crouse, J. D., Wennberg, P. O., Keller, C. A., Hudman, R. C., Barkley, M. P., and Horowitz, L. W.: Ozone and organic nitrates over the eastern United States: Sensitivity to isoprene chemistry, 118, 11,256–11,268, <https://doi.org/10.1002/jgrd.50817>, 2013.
- 830 Müller, M., Mikoviny, T., Feil, S., Haidacher, S., Hanel, G., Hartungen, E., Jordan, A., Märk, L., Mutschlechner, P., Schottkowsky, R., Sulzer, P., Crawford, J. H., and Wisthaler, A.: A compact PTR-ToF-MS instrument for airborne measurements of volatile organic compounds at high spatiotemporal resolution, 7, 3763–3772, <https://doi.org/10.5194/amt-7-3763-2014>, 2014.
- 835 O'Dell, K., Ford, B., Fischer, E. V., and Pierce, J. R.: Contribution of Wildland-Fire Smoke to US PM_{2.5} and Its Influence on Recent Trends, *Environ. Sci. Technol.*, 53, 1797–1804, <https://doi.org/10.1021/acs.est.8b05430>, 2019.
- 840 Pfannerstill, E. Y., Reijrink, N. G., Edtbauer, A., Ringsdorf, A., Zannoni, N., Araújo, A., Ditas, F., Holanda, B. A., Sá, M. O., Tsokankunku, A., Walter, D., Wolff, S., Lavrič, J. V., Pöhlker, C., Sörgel, M., and Williams, J.: Total OH reactivity over the Amazon rainforest: variability with temperature, wind, rain, altitude, time of day, season, and an overall budget closure, 21, 6231–6256, <https://doi.org/10.5194/acp-21-6231-2021>, 2021.
- Philip, S., Martin, R. V., and Keller, C. A.: Sensitivity of chemistry-transport model simulations to the duration of chemical and transport operators: a case study with GEOS-Chem v10-01, 9, 1683–1695, <https://doi.org/10.5194/gmd-9-1683-2016>, 2016.
- 845 Rastigejev, Y., Park, R., Brenner, M. P., and Jacob, D. J.: Resolving intercontinental pollution plumes in global models of atmospheric transport, 115, <https://doi.org/10.1029/2009JD012568>, 2010.
- 850 Reddington, C. L., Spracklen, D. V., Artaxo, P., Ridley, D. A., Rizzo, L. V., and Arana, A.: Analysis of particulate emissions from tropical biomass burning using a global aerosol model and long-term surface observations, 16, 11083–11106, 2016.
- Reddington, C. L., Morgan, W. T., Darbyshire, E., Brito, J., Coe, H., Artaxo, P., Scott, C. E., Marsham, J., and Spracklen, D. V.: Biomass burning aerosol over the Amazon: analysis of aircraft, surface and satellite observations using a global aerosol model, *Atmos. Chem. Phys.*, 19, 9125–9152, <https://doi.org/10.5194/acp-19-9125-2019>, 2019.
- 855 Robinson, A. L., Donahue, N. M., Shrivastava, M. K., Weitkamp, E. A., Sage, A. M., Grieshop, A. P., Lane, T. E., Pierce, J. R., and Pandis, S. N.: Rethinking Organic Aerosols: Semivolatile Emissions and Photochemical Aging, 315, 1259–1262, <https://doi.org/10.1126/science.1133061>, 2007.



- 860 Safieddine, S. A., Heald, C. L., and Henderson, B. H.: The global nonmethane reactive organic carbon budget: A modeling perspective, *Geophys. Res. Lett.*, 44, 3897–3906, <https://doi.org/10.1002/2017GL072602>, 2017.
- Senande-Rivera, M., Insua-Costa, D., and Miguez-Macho, G.: Spatial and temporal expansion of global wildland fire activity in response to climate change, *Nat Commun*, 13, 1208, <https://doi.org/10.1038/s41467-022-28835-2>, 2022.
- 865 Sherwen, T., Schmidt, J. A., Evans, M. J., Carpenter, L. J., Großmann, K., Eastham, S. D., Jacob, D. J., Dix, B., Koenig, T. K., Sinreich, R., Ortega, I., Volkamer, R., Saiz-Lopez, A., Prados-Roman, C., Mahajan, A. S., and Ordóñez, C.: Global impacts of tropospheric halogens (Cl, Br, I) on oxidants and composition in GEOS-Chem, 16, 12239–12271, <https://doi.org/10.5194/acp-16-12239-2016>, 2016.
- 870 Simone, N. W., Stettler, M. E. J., and Barrett, S. R. H.: Rapid estimation of global civil aviation emissions with uncertainty quantification, *Transportation Research Part D: Transport and Environment*, 25, 33–41, <https://doi.org/10.1016/j.trd.2013.07.001>, 2013.
- 875 Simpson, I. J., Akagi, S. K., Barletta, B., Blake, N. J., Choi, Y., Diskin, G. S., Fried, A., Fuelberg, H. E., Meinardi, S., Rowland, F. S., Vay, S. A., Weinheimer, A. J., Wennberg, P. O., Wiebring, P., Wisthaler, A., Yang, M., Yokelson, R. J., and Blake, D. R.: Boreal forest fire emissions in fresh Canadian smoke plumes: C₁-C₁₀; volatile organic compounds (VOCs), CO₂, CO, NO₂, NO, HCN and CH₃CN, *Atmos. Chem. Phys.*, 11, 6445–6463, <https://doi.org/10.5194/acp-11-6445-2011>, 2011.
- 880 Sinha, V., Williams, J., Crowley, J. N., and Lelieveld, J.: The Comparative Reactivity Method – a new tool to measure total OH Reactivity in ambient air, 8, 2213–2227, <https://doi.org/10.5194/acp-8-2213-2008>, 2008.
- 885 Stettler, M. E. J., Eastham, S., and Barrett, S. R. H.: Air quality and public health impacts of UK airports. Part I: Emissions, *Atmospheric Environment*, 45, 5415–5424, <https://doi.org/10.1016/j.atmosenv.2011.07.012>, 2011.
- 890 Stockwell, C. E., Bela, M. M., Coggon, M. M., Gkatzelis, G. I., Wiggins, E., Gargulinski, E. M., Shingler, T., Fenn, M., Griffin, D., Holmes, C. D., Ye, X., Saide, P. E., Bourgeois, I., Peischl, J., Womack, C. C., Washenfelder, R. A., Veres, P. R., Neuman, J. A., Gilman, J. B., Lamplugh, A., Schwantes, R. H., McKeen, S. A., Wisthaler, A., Piel, F., Guo, H., Campuzano-Jost, P., Jimenez, J. L., Fried, A., Hanisco, T. F., Huey, L. G., Perring, A., Katich, J. M., Diskin, G. S., Nowak, J. B., Bui, T. P., Halliday, H. S., DiGangi, J. P., Pereira, G., James, E. P., Ahmadov, R., McLinden, C. A., Soja, A. J., Moore, R. H., Hair, J. W., and Warneke, C.: Airborne Emission Rate Measurements Validate Remote Sensing Observations and Emission Inventories of Western U.S. Wildfires, *Environ. Sci. Technol.*, <https://doi.org/10.1021/acs.est.1c07121>, 2022.
- 895 Strode, S. A., Liu, J., Lait, L., Commane, R., Daube, B., Wofsy, S., Conaty, A., Newman, P., and Prather, M.: Forecasting carbon monoxide on a global scale for the ATom-1 aircraft mission: insights from airborne and satellite observations and modeling, 18, 10955–10971, <https://doi.org/10.5194/acp-18-10955-2018>, 2018.



- 900 Taraborrelli, D., Cabrera-Perez, D., Bacer, S., Gromov, S., Lelieveld, J., Sander, R., and Pozzer, A.: Influence of aromatics on tropospheric gas-phase composition, 21, 2615–2636, <https://doi.org/10.5194/acp-21-2615-2021>, 2021.
- 905 Travis, K. R., Jacob, D. J., Fisher, J. A., Kim, P. S., Marais, E. A., Zhu, L., Yu, K., Miller, C. C., Yantosca, R. M., Sulprizio, M. P., Thompson, A. M., Wennberg, P. O., Crouse, J. D., St Clair, J. M., Cohen, R. C., Laughner, J. L., Dibb, J. E., Hall, S. R., Ullmann, K., Wolfe, G. M., Pollack, I. B., Peischl, J., Neuman, J. A., and Zhou, X.: Why do Models Overestimate Surface Ozone in the Southeastern United States?, *Atmos Chem Phys*, 16, 13561–13577, <https://doi.org/10.5194/acp-16-13561-2016>, 2016.
- 910 Voulgarakis, A., Naik, V., Lamarque, J.-F., Shindell, D. T., Young, P. J., Prather, M. J., Wild, O., Field, R. D., Bergmann, D., Cameron-Smith, P., Cionni, I., Collins, W. J., Dalsøren, S. B., Doherty, R. M., Eyring, V., Faluvegi, G., Folberth, G. A., Horowitz, L. W., Josse, B., MacKenzie, I. A., Nagashima, T., Plummer, D. A., Righi, M., Rumbold, S. T., Stevenson, D. S., Strode, S. A., Sudo, K., Szopa, S., and Zeng, G.: Analysis of present day and future OH and methane lifetime in the ACCMIP simulations, 13, 2563–2587, <https://doi.org/10.5194/acp-13-2563-2013>, 2013.
- 915 Wang, S., Coggon, M. M., Gkatzelis, G. I., Warneke, C., Bourgeois, I., Ryerson, T., Peischl, J., Veres, P. R., Neuman, J. A., Hair, J., Shingler, T., Fenn, M., Diskin, G., Huey, L. G., Lee, Y. R., Apel, E. C., Hornbrook, R. S., Hills, A. J., Hall, S. R., Ullmann, K., Bela, M. M., Trainer, M. K., Kumar, R., Orlando, J. J., Flocke, F. M., and Emmons, L. K.: Chemical Tomography in a Fresh Wildland Fire Plume: A Large Eddy Simulation (LES) Study, *JGR Atmospheres*, 126, <https://doi.org/10.1029/2021JD035203>, 2021.
- 920 van der Werf, G. R., Randerson, J. T., Giglio, L., van Leeuwen, T. T., Chen, Y., Rogers, B. M., Mu, M., van Marle, M. J. E., Morton, D. C., Collatz, G. J., Yokelson, R. J., and Kasibhatla, P. S.: Global fire emissions estimates during 1997–2016, 9, 697–720, <https://doi.org/10.5194/essd-9-697-2017>, 2017.
- 925 Westerling, A. L.: Increasing western US forest wildfire activity: sensitivity to changes in the timing of spring, *Phil. Trans. R. Soc. B*, 371, 20150178, <https://doi.org/10.1098/rstb.2015.0178>, 2016.
- 930 Westerling, A. L., Hidalgo, H. G., Cayan, D. R., and Swetnam, T. W.: Warming and Earlier Spring Increase Western U.S. Forest Wildfire Activity, 313, 940–943, <https://doi.org/10.1126/science.1128834>, 2006.
- Wiedinmyer, C., Akagi, S., Yokelson, R., Emmons, L., Al-Saadi, J., Orlando, J., and Soja, A.: The Fire INventory from NCAR (FINN): A High Resolution Global Model to Estimate the Emissions from Open Burning, 625–641, 2011.
- 935 Wiedinmyer, C., Yokelson, R. J., and Gullett, B. K.: Global Emissions of Trace Gases, Particulate Matter, and Hazardous Air Pollutants from Open Burning of Domestic Waste, *Environ. Sci. Technol.*, 48, 9523–9530, <https://doi.org/10.1021/es502250z>, 2014.



- Wisthaler, A., Hansel, A., Dickerson, R. R., and Crutzen, P. J.: Organic trace gas measurements by PTR-MS during INDOEX 1999, 107, INX2 23-1-INX2 23-11, <https://doi.org/10.1029/2001JD000576>, 2002.
- 940 Xu, L., Crounse, J. D., Vasquez, K. T., Allen, H., Wennberg, P. O., Bourgeois, I., Brown, S. S., Campuzano-Jost, P., Coggon, M. M., Crawford, J. H., DiGangi, J. P., Diskin, G. S., Fried, A., Gargulinski, E. M., Gilman, J. B., Gkatzelis, G. I., Guo, H., Hair, J. W., Hall, S. R., Halliday, H. A., Hanisco, T. F., Hannun, R. A., Holmes, C. D., Huey, L. G., Jimenez, J. L., Lamplugh, A., Lee, Y. R., Liao, J., Lindaas, J., Neuman, J. A., Nowak, J. B., Peischl, J., Peterson, D. A., Piel,
945 F., Richter, D., Rickly, P. S., Robinson, M. A., Rollins, A. W., Ryerson, T. B., Sekimoto, K., Selimovic, V., Shingler, T., Soja, A. J., Clair, J. M. S., Tanner, D. J., Ullmann, K., Veres, P. R., Walega, J., Warneke, C., Washenfelder, R. A., Weibring, P., Wisthaler, A., Wolfe, G. M., Womack, C. C., and Yokelson, R. J.: Ozone chemistry in western U.S. wildfire plumes, <https://doi.org/10.1126/sciadv.abl3648>, 2021.
- 950 Yang, Y., Shao, M., Wang, X., Nölscher, A. C., Kessel, S., Guenther, A., and Williams, J.: Towards a quantitative understanding of total OH reactivity: A review, *Atmospheric Environment*, 134, 147–161, <https://doi.org/10.1016/j.atmosenv.2016.03.010>, 2016.
- Yokelson, R. J., Christian, T. J., Karl, T. G., and Guenther, A.: The tropical forest and fire emissions experiment: laboratory fire measurements and synthesis of campaign data, 8, 3509–
955 3527, <https://doi.org/10.5194/acp-8-3509-2008>, 2008.
- Yokelson, R. J., Crounse, J. D., DeCarlo, P. F., Karl, T., Urbanski, S., Atlas, E., Campos, T., Shinozuka, Y., Kapustin, V., Clarke, A. D., Weinheimer, A., Knapp, D. J., Montzka, D. D., Holloway, J., Weibring, P., Flocke, F., Zheng, W., Toohey, D., Wennberg, P. O., Wiedinmyer, C., Mauldin, L., Fried, A., Richter, D., Walega, J., Jimenez, J. L., Adachi, K., Buseck, P. R.,
960 Hall, S. R., and Shetter, R.: Emissions from biomass burning in the Yucatan, 28, 2009.
- Zhang, L., Jacob, D. J., Yue, X., Downey, N. V., Wood, D. A., and Blewitt, D.: Sources contributing to background surface ozone in the US Intermountain West, 14, 5295–5309, <https://doi.org/10.5194/acp-14-5295-2014>, 2014.
- 965 Zhao, X. and Wang, L.: Atmospheric Oxidation Mechanism of Furfural Initiated by Hydroxyl Radicals, *J. Phys. Chem. A*, 121, 3247–3253, <https://doi.org/10.1021/acs.jpca.7b00506>, 2017.